J Fluoresc (2008) 18:827–833
DOI 10.1007/s10895-008-0311-8

ORIGINAL PAPER

Determination of Enoxacin Using Tb Composite Nanoparticles Sensitized Luminescence Method

Mohammad Mainul Karim · Sang Hak Lee

Received: 30 October 2007 / Accepted: 2 January 2008 / Published online: 16 January 2008

Abstract In our study, terbium-acetylacetone (Tb-acac) composite nanoparticles have been prepared under vigorous ultrasonic irradiation. The nanoparticles are water soluble, stable and have extremely narrow emission bands and high internal quantum efficiencies. They were used as fluorescence probes in the determination of enoxacin (Enox) based on the fluorescence enhancement of nanoparticles through fluorescence resonance energy transfer (FRET). The influence of buffer solution on the fluorescence intensity was investigated. Under the optimum conditions, the fluorescence intensity of the Tb-acac-Enox system is linearly proportional to the Enox concentration in the Enox concentration range of 2×10^{-7}–1×10^{-4} M. The correlation coefficient for the calibration curve was 0.9976. The limit of detection as defined by IUPAC, $C_{LOD}=3S_b/m$ (where S_b is the standard deviation of the blank signals and m is the slope of the calibration graph) was found to be 3×10^{-8} M. The relative standard deviation (RSD) for six repeated measurements of 1×10^{-4} M Enox was 1.35%. The method was applied to the determination of Enox in pharmaceutical formulation and recovery results were obtained from urine samples.

Keywords Enoxacin · Fluorescence resonance energy transfer · Terbium composite nanoparticles · Acetylacetone

Introduction

Enoxacin (Enox), an antibiotic in the class of fluoroquinolone drugs, is used in the treatment of urinary tract, respiratory, gastro-intestinal and skin infections because of its excellent activity against bacteria, low frequency of adverse effect and good absorption on oral administration. Structurally (Fig. 1), it is an amino compound containing piperazine moiety at 7 and fluorine at 6 positions. Fluorine at position 6 confers greater antibacterial potency and piperazine moiety at position 7 confers antipseudomonal activity [1]. The extensive use of this compound and the need for clinical and pharmacological study require fast and sensitive analytical techniques for determination of its presence in biological fluids and pharmaceutical formulations. Numerous methods have been reported for the determination of Enox including differential pulse polarography [2], single-sweep polarography [3], reversed-phase high-performance liquid chromatography [4], capillary electrophoresis using solid-phase extraction [5], liquid chromatography–tandem mass spectrometry [6], spectrophotometric [7], micellar liquid chromatography [8], HPLC-PIF [9]. Electrochemiluminescence using Tb^{3+}-Enox-Na_2SO_3 system [10] and chemiluminescence using $KMnO_4$-Na_2SO_3-Tb^{3+}-Enox [11] and $Ru(phen)_3^{2+}$−Ce(IV)[12] for Enox determination have already been reported.

In contrast, fluorimetry is a simple and highly sensitive method for the assay of a large number of drugs and metals [13–16] and fluorimetric-based chemo-sensor is a very interesting category for future practical applications, thanks to the sensitivity, specificity, and low costs of fluorescence measurements. Two fluorimetric techniques using partial least squares multi component analysis [17] and terbium sensitizing luminescence [18] were reported for the assay of Enox.

Fluorimetric nanoparticles are gaining much attention in analytical chemistry because of their unique properties originating from the quantum size effect and they are significantly different from those of the corresponding bulk materials in terms of sensitivity. Inorganic nanoparticles

M. M. Karim · S. H. Lee (✉)
Department of Chemistry, Kyungpook National University, Taegu 702-701, South Korea
e-mail: shlee@knu.ac.kr

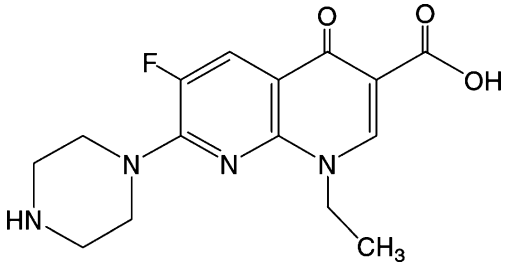

Fig. 1 Structure of enoxacin

have certain advantages of brightness, strong stability against photobleaching and resistance to blinking [19]. They have been extensively investigated for various potential applications including the fluorescent biological labels, photovoltaic cells, light-emitting diodes and optical sensors. As far as the application is concerned, fluorescent inorganic nanoparticles such as ZnS, ZnSe, CdS, CdTe and CdSe need complication procedures for surface modification in order to make them water soluble and biocompatible. Therefore, it is still a big challenge to prepare water soluble, biocompsitable and monodisperse nanoparticles used for biochemical probes and sensors.

Composite nanoparticle materials have attracted the interest of a number of researchers, because of their hybrid and synergistic properties derived from several components, either in bulk or in solution, these materials provide unique electrical and optical properties [20, 21]. It is reported that the nanoparticle probes are brighter, more stable against photobleaching, and do not suffer from blinking in comparison with single organic fluorophores [22]. So, there has been increasing interest in the design and synthesis of nanoparticles as probe for the application in biochemistry [23, 24].

The narrow line luminescence of terbium ions makes them important components in energy-efficient optical devices [25]. Lanthanides in aqueous solution are known to be either non-fluorescent or weakly fluorescent due to their low molar absorptivities and poor quantum yields [26]. The problem due to low molar absorptivity is overcome by employing the technique of ligand-sensitized fluorescence. In this technique, the weakly fluorescent lanthanide ion is complexed with a ligand of higher molar absorptivity. Then the ligand is excited in its absorption band. Some of the excited energy from the ligand is transferred to the lanthanide ion by intramolecular energy transfer. Various ligands have been used to sensitize and enhance lanthanide fluorescence [27, 28].

In this work, we have synthesized Tb-acetylacetone (Tb-acac) composite nanoparticles using the ultrasonic method. Ultrasonic irradiation can be used extensively to generate novel materials with unusual properties; because ultrasonic irradiation causes the formation of particles with much smaller and higher surface area [29]. We used acetylacetone (acac) which has high absorptivity as ligand. The nanoparticles are water soluble, stable and have extremely narrow emission bands and high internal quantum efficiencies. They were used as fluorescence probes in the determination of Enox based on the fluorescence enhancement of nanoparticles through fluorescence resonance energy transfer (FRET). The influence of buffer solution on the fluorescence intensity was investigated. Under the optimum conditions, the fluorescence intensity of Tb-composite nanoparticle-Enox is linearly proportional to Enox concentration in the Enox concentration range of 2×10^{-7} to 1×10^{-4} M. The limit of detection was found to be 3×10^{-8} M. The relative standard deviation (RSD) for 6 repeated measurements of 1×10^{-4} M Enox was 1.35%. The method was applied to the determination of Enox in pharmaceutical formulation and recovery results were obtained from the urine samples.

Experimental

Reagents

All experiments were performed with analytical-reagent grade chemicals and pure solvents. Doubly distilled and dematerialized water was used throughout. Stock solution of Enox was prepared by dissolving the corresponding Enox in water; working solutions were prepared by appropriate dilution with water. Enox solutions were preserved in refrigerator when not in use. $TbCl_3$ solution of 1×10^{-2} M was prepared by dissolving terbium(III) chloride hexahydrate (99.9%, Aldrich, USA) in doubly distilled water. Acetylacetone (acac) (≥99%, Sigma-Aldrich, Inc. USA) was distilled just before use and prepared in ethyl alcohol. Potassium persulfate (KSP) was acquired from Acros. Phosphate buffer solution of pH=7.2 was prepared as follows: 36.0 ml of 0.2 M Na_2HPO_4 and 14 ml of 0.2 M NaH_2PO_4 were transferred into a 100 ml standard flask and diluted to the mark with water.

Apparatus

All the spectrofluorimetric measurements were conducted with a SPEX Fluorolog-2 spectrofluorometer (Model F111, SPEX industries, Edison, NJ, USA). The spectrometer used a 450-W Xenon lamp (Model XBO 450 W/1, Osram, Germany) as the excitation light source and a photomultiplier tube (Model R928, Hamamatsu, Japan) powered at 950 V as the detector. Excitation and emission monochromator slit, increment, and integration time were set at 1 mm, 1 nm and 1 second, respectively. All spectral data were obtained by SPEX DM 3000F spectroscopy computer. A pH meter (Model 520A, Orion, USA) was used for pH

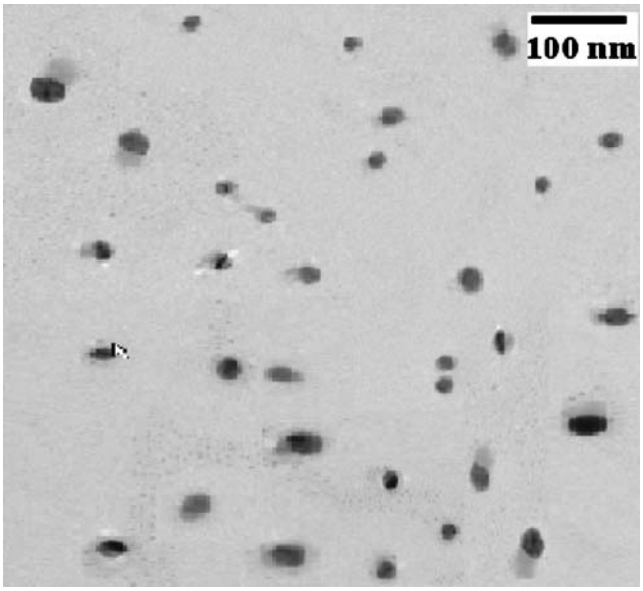

Fig. 2 TEM image of Tb-acac composite nanoparticles

measurements. An ultrasonic generator (Model ULH 7005, Ulsso Hi-Tech Co., Ltd, Korea) was used in the ultrasonic preparation of composite nanoparticles. The sample for transmission electron microscopic (TEM) observation was prepared by doping the dispersion on a copper grid to observe the morphology of composite particle by TEM (Model CM-30, Phillips, New York, USA) with an accelerating voltage of 100 kV.

Procedure

The Tb-acac composite nanoparticles were prepared as follows [30]. The synthesis of the composite nanoparticles was performed in a 1 L three-necked round-bottomed flask. About 620 ml water and 13.0 ml of 1×10^{-2} M $TbCl_3$ were

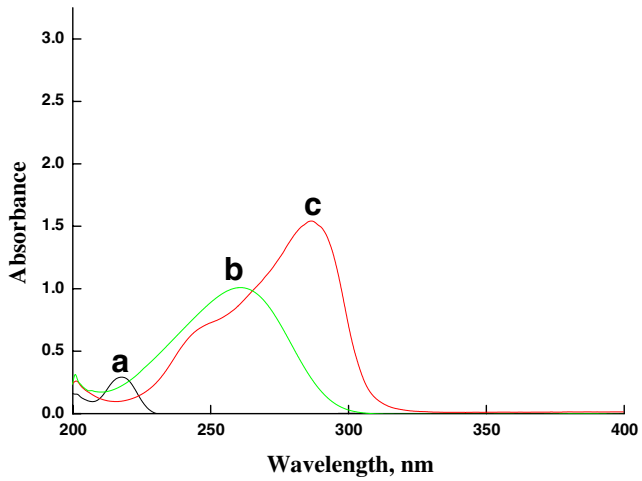

Fig. 3 UV-visible absorption spectra of **a** Tb, **b** Acac in aqueous solution and **c** Tb-acac composite nanoparticles dispersed in aqueous solution with particle size ≈25 nm. (represented by the concentration of Tb-acac existing in single molecules)

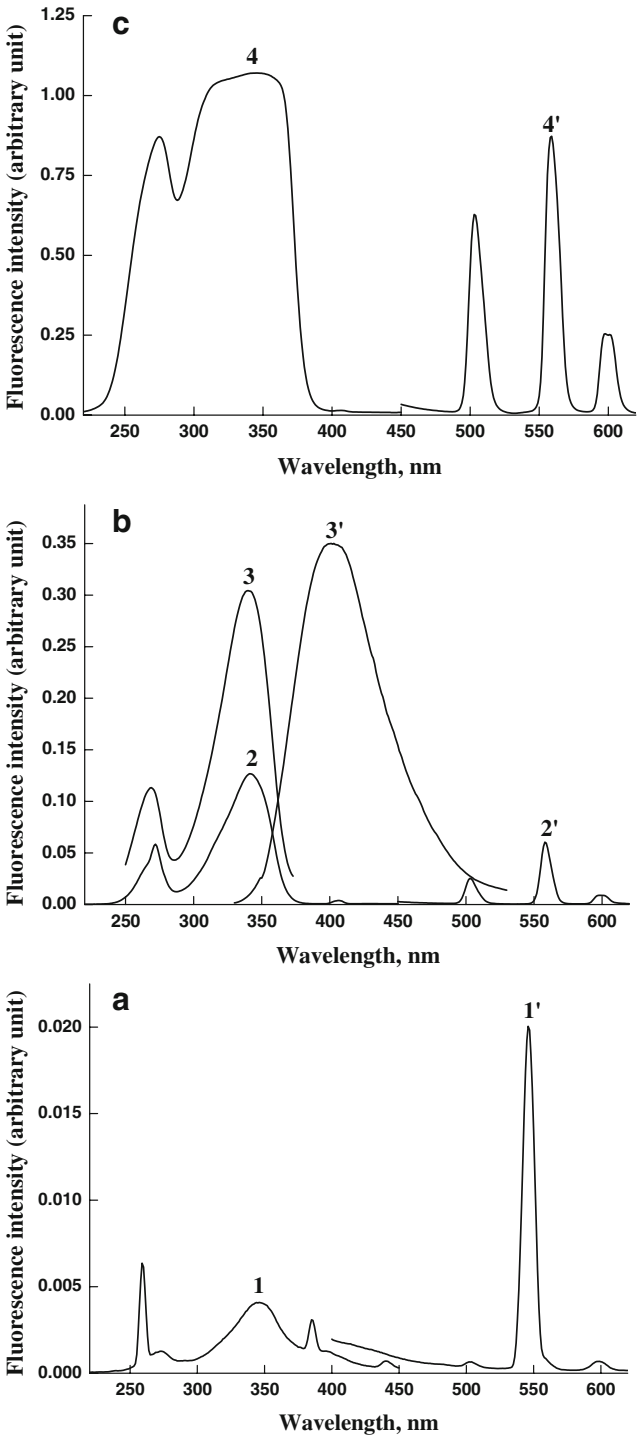

Fig. 4 **a** Excitation (*1*) and emission (*1′*) spectra of Tb^{3+}: $[Tb^{3+}] = 3\times10^{-4}$ M, $\lambda_{ex}/\lambda_{em} = 345/545$. **b** Excitation (*2*, *3*) and emission (2′, 3′) spectra of Tb-acac composite nanoparticle and Enox: [Tb – acac composite nanoparticle] $= 3\times10^{-4}$ M, $\lambda_{ex}/\lambda_{em} = 345/559$, pH 7.2, [Enox] $= 1\times10^{-4}$ M, $\lambda_{ex}/\lambda_{em} = 339/402$. **c** Excitation (*4*) and emission (*4′*) spectra of Tb-composite nanoparticle in the presence of Enox. [Tb – acac composite nanoparticle] $= 3\times10^{-4}$ M, [Enox] $= 1\times10^{-4}$ M, pH 7.2, $\lambda_{ex}/\lambda_{em} = 345/559$

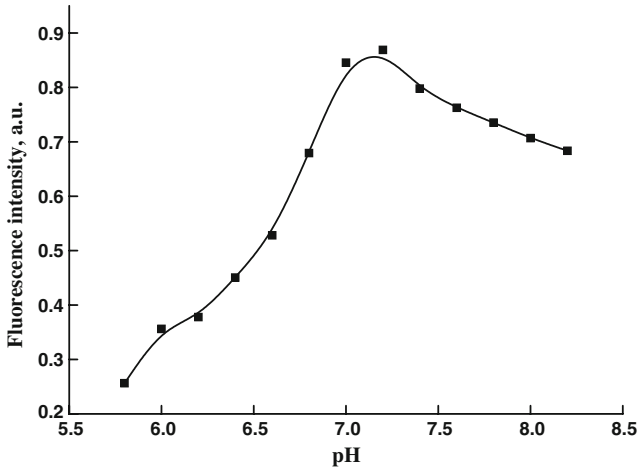

Fig. 5 Effect of pH on the fluorescence intensity of Tb-acac composite nanoparticles in the presence of Enox: [Enox] = 1×10^{-4} M, $[Tb^{3+}] = 3 \times 10^{-4}$ M (represented by the concentration of Tb^{3+}-acac existing in single molecule), $\lambda_{ex}/\lambda_{em} = 345/559$

added into the flask respectively. Under vigorous stirring, 6.5 ml of 6×10^{-2} M acac and then 0.0004 g KSP were added to the mixture drop wise. pH was adjusted to about 7.5 with 0.1 M NaOH. The composite nanoparticles were prepared under ultrasonic irradiation within 30 min. Before being irradiated with 20 kHz output frequency at 700 W output power, the flask was purged with nitrogen to eliminate the oxygen in it.

The nanoparticles are water soluble and stable at room temperature for at least 1 month. The nanoparticles were used as the fluorimetric probes for the determination of Enox. The following procedure was adopted. To a 10 ml volumetric flask, 2.0 ml of buffer (pH=7.2), a certain volume of nanoparticles, and an appropriate volume of Enox was added. The mixture was diluted to the volume with water and mixed before the fluorescence intensity was measured. The excitation wavelength was set at 345 nm and the emission wavelength at 559 nm.

Results and discussion

TEM image and UV spectral characteristics

In order to investigate the particle size the image of terbium composite nanoparticles was obtained by using transmission electron microscopy (TEM) as shown in Fig. 2. TEM was recorded on Phillips CM-30 with an accelerating voltage of 100 kV. Samples were dispersed in ethanol and dispersion was dropped on copper grid. From the Fig. 2 the average diameter of the Tb-acac composite nanoparticles is about 25 nm. In addition, the TEM image shows that the nanoparticles are homogeneously distributed and not aggregated. It has been known that the sonochemical reaction occurs in solution, yielding Tb-acac nanoparticles, because the $TbCl_3$ and acac may well react with under the extreme conditions of sonification. Ultrasonic waves are intense enough to produce cavitation that can drive chemical reactions [31].

In order to get the idea about the formation of composite nanoparticles in solution, the ultrasonic irradiated solution was taken out at different sonication times for the absorption spectrum measurement and the spectrum was compared with that of terbium and acac. Figure 3 displays the UV-visible absorption spectra of terbium, acac, and terbium-acac composite nanoparticle with particle size about 25 nm. Aqueous solution of terbium has low absorption peak at 217 nm and acac has characteristic peak at 260 nm. It can be observed that at sonication time of 30 min, the spectrum of terbium composite nanoparticle has two clearly resolved peaks at 244 and 286 nm, which can be indicative of formation and an increase in the amount of terbium composite nanoparticles in the solution.

Characteristics of fluorescence spectra

In order to investigate the spectral characteristics, excitation and emission spectra of Tb^{3+}, Enox, Tb^{3+}-acac composite nanoparticles and Tb^{3+}-acac composite nanoparticles in the presence of Enox were recorded in solution at pH of 7.2 using SPEX Fluorolog-2 spectrofluorometer; the concentrations of Tb^{3+} (represented by the concentration of Tb^{3+}-acac existing in single molecule) and Enox were fixed at 3×10^{-4} M and 1×10^{-4} M, respectively. Final excitation and emission maxima selected for calibration of Enox were 345 nm and 559 nm, respectively. Figure 4a (1′) shows the week emission peak of Tb at 545 nm when excited at 345 nm (1) shown in Fig. 4a. In order to avoid direct excitation of Tb^{3+} [32], the disturbance of the scattered excitation light and the inner filter effect [33] we selected

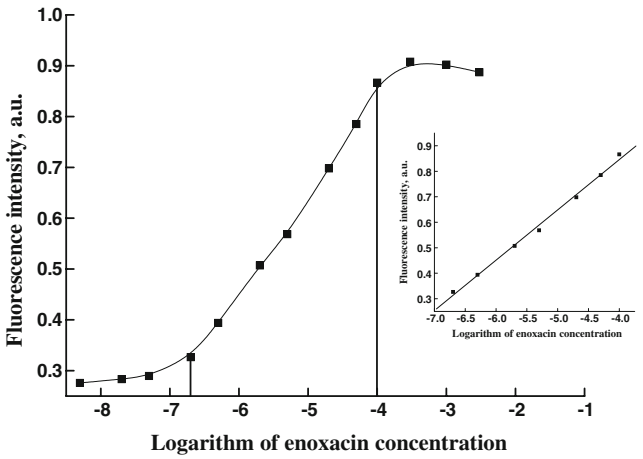

Fig. 6 Calibration curve for enoxacin. *Inset* Linearity of the calibration curve. The other conditions are the same as those in Fig. 5

Table 1 Effect of interfering substances

Interferents	Tolerable concentration (M)	Change in FL intensity (F%)
Ibuprofen and cimetidine	5.5×10^{-4}	1.5
Amoxicillin	5×10^{-4}	4.5
Zn^{2+}, K^{+}, NH^{4+}, Ca^{2+}, Mg^{2+}, Na^{+}, Al^{3+}, Pb^{2+}, Ni^{2}, $Mn^{2+}$and Fe^{3+}	4×10^{-3}	2.31
Dextrine, glucose and starch	1.2×10^{-3}	3.21
Vitamin B_1	2.5×10^{-3}	1.75
Hemoglobin and myoglobin	3×10^{-3}	−2.00
Co^{2+} and Cu^{2+}	2.5×10^{-3}	−4.5
Uric acid and boric acid	1.5×10^{-5}	0.5

345 nm rather than 259 nm. As can be seen in Fig. 4b the emission spectrum (3′) of Enox is overlapped with the excitation spectrum of Tb (2).

Tb-acac composite nanoparticles show the emission band at 559 nm (spectrum 2′) at excitation wavelength of 345 nm (spectrum 2), as shown in Fig. 4b. It can be seen that the emission intensity of composite nanoparticle was three times higher than the emission intensity of Tb^{3+}. In comparison with spectrum 2′ (the emission spectrum of Tb-acac) shown in Fig. 4b, spectrum 4′ shown in Fig. 4c clearly indicates that emission intensity of Tb-acac composite nanoparticle at 559 nm increases drastically (about 15-fold) in the presence of Enox when excited at 345 nm (spectrum 4). It can be observed that the most intense band located at 559 nm, so 559 nm was selected for the emission wavelength. The results show that the broad emission band of Enox decreases, while the narrower emission band of Tb^{3+} appears after Enox was added to the Tb-acac composite nanoparticle solution. The emission intensity is also more intense than that of uncomplexed Enox. Therefore, it is feasible to determine Enox by terbium-composite nanoparticle-sensitized luminescence method.

Based on the experiment it can be suggested that Enox is an ideal ligand for Tb^{3+} ion and it is possible to sensitize the fluorescence intensity of Tb-acac composite nanoparticles via intramolecular energy transfer [34]. According to the Förster non-radiation energy transfer theory [35], the rate of energy transfer depends upon the extent of overlap of the emission spectra of the donor with the excitation spectra of the accepter and the distance between molecules. Energy transfer easily occurred between Enox and Tb^{3+}-composite because of the spectral overlap between the fluorescence spectra of donor (Enox) and the excitation spectra of accepter (Tb-acac).

It can be further mentioned that the coordination number of Tb^{3+} is generally eight [36]. It can be suggested that there are still a lot of positive charges and blank orbits in Tb^{3+}. Because Enox exists as an anionic state in solution, it can combine with the composite nanoparticle via electrostatic interaction. Because of the effect of packing and cooperation in the ternary complex, the energy transfer can more easily occur and the non-radioactive energy loss can be decreased greatly. So the fluorescence intensity of Tb^{3+} at 559 nm can be enhanced several times.

Effect of pH

To find the optimum pH of the sample solution for the determination of Enox the effect of pH on the fluorescence intensity obtained from the Tb-acac composite nanoparticles-Enox was investigated. The concentration used for Enox was 1×10^{-4} M. The concentration of Tb^{3+} (represented by the concentration of Tb^{3+}-acac existing in single molecule) was selected as 3×10^{-4} M. The fluorescence intensity was examined over the pH range from 5.8 to 8.2. The pH of buffer solution was adjusted by 0.2 M Na_2HPO_4 and 0.2 M NaH_2PO_4 solutions. The volume of added buffer was fixed to 2 ml. The results of pH effect are shown in Fig. 5. The figure shows that the

Table 2 Results for the assay of Enox in tablet (n=3)

Sample	Amount found± RSD (%)		Enox added ($\times10^{-5}$ M)	Enox found ($\times10^{-5}$ M)	Recovery± RSD (%)
	Labeled	Method			
Enox	100[a]	99.85±2.3	2	1.96	98.0±1.3
			5	4.93	98.6±2.6
			7	6.79	97±2.0

[a] Content of active ingredient in 200 mg tablet powder

Table 3 Results of assay of Enox in urine sample (n=4)

Urine sample	Real sample ($\times10^{-5}$ M)	Recovery		
		Enox added ($\times10^{-6}$ M)	Enox found ($\times10^{-6}$ M)	Recovery± RSD (%)
Enox	6.21±1.19	2	1.89	94.5±2.6
		3	2.88	96±3.2
		5	4.93	98.6±2.5
		10	9.87	98.7±3.5

fluorescence intensity increases up to pH 7.2. The intensity increases with pH increasing when pH<7.2 because the increase of $-COO^-$ of Enox enhances the formation of Tb^{3+} composite-Enox complex. Further increase in pH value decreases the fluorescence intensity of system. As the volume of buffer solution added from 0.5 to 3.0 ml, fluorescence intensity reached maximum at 2.0 ml for the buffer and remained constant up to the volume 3 ml, and then 2 ml buffer was chosen in the following experiments.

Calibration for enoxacin

In order to evaluate analytical characteristics of this method, we obtained the calibration curve by plotting logarithm of the Enox concentration versus fluorescence intensity. 13 standard solutions were prepared for the calibration curve. These were the optimum conditions: Tb^{3+}, 3×10^{-4} M (represented by the concentration of Tb^{3+}-acac existing in single molecule) and pH 7.2. The calibration curve showed (Fig. 6) a linear relationship over Enox concentration of 2×10^{-7}–1×10^{-4} M. Above this concentration the inner filter effect and /or quenching are apparently causing some deviation from linearity [37]. The linear regression analysis using the method of least square treatment of calibration data (n=7) was made to evaluate slope, intercept and correlation coefficient. The regression of log[X] versus fluorescence intensity (Y) gave the following linear regression equation:

$$Y = 3.271\text{E}7 + 3.948\text{E}6\ \text{Log}[X]$$

with a correlation coefficient (R) of 0.9976. The limit of detection as defined by IUPAC, $C_{LOD}=3S_b/m$ (where S_b is the standard deviation of the blank signals and m is the slope of the calibration graph) was found to be 3×10^{-8} M. The relative standard deviation (RSD) for six repeated measurements of 1×10^{-4} M Enox was 1.35%.

Interferences

In a real sample, the analyte under investigation will be in the presence of interferents. They may suppress or enhance the fluorescence signal, although they have no significant effect on the intensity. Effect of potential interfering substances was investigated by preparing a set of solutions, each one with 1.0×10^{-5} M Enox plus a different concentration of a chemical species to be tested. The experimental results are shown in Table 1. A chemical species is considered as non-interfering when its effect on the fluorescence signal of the Tb-composite-Enox system is less than 5% deviation. Possible interference from uric acid can be eliminated by diluting urine sample. Therefore, the effects of these possible interferents could be ignored.

Analytical application

We tested the application of our proposed method by using it for the practical analyses of Enox in pharmaceutical formulation and urine sample. Five tablets (for Enox) were weighed and ground. An accurately weighed amount of 200 mg for Enox powder was transferred into a beaker. The powder was dissolved with DI water, and the solution was filtered. Finally the solution was diluted appropriately to meet the linear range. No further pretreatment was needed for urine samples except proper dilution. According to the basic procedure enoxacin was determined from the tablet solution and the results are shown in Table 2. As can be seen, there is no significant difference between labeled value and that obtained by the proposed method. Recovery ranges from 97–98.6%. A healthy volunteer administered 200 mg Enox and then after 12 h the real urine samples were analyzed. Urine samples were properly diluted in order to make the concentrations of the drug within the working range, and then measured by the standard addition method. The results are given in Table 3.

Conclusions

We described a simple assay of Enox based on Tb-composite nanoparticle sensitized luminescence method. The fluorescence of Tb-acac at 559 nm is sensitized because of fluorescence resonance energy transfer between the donor (Enox) and acceptor (Tb-acac). The method provides a wide dynamic range of 2×10^{-7}–1×10^{-4} M Enox. To evaluate the factors that affect the sensitivity of detection, the concentration Tb-acac and the pH of the solution have been optimized. In addition, the method estimated the concentration of Enox in urine sample. Some potential advantages can be summarized from the proposed method: (1) All experiments can be performed in aqueous solution (2) Pretreatment of real sample is not required (3) Tb-acac composite nanoparticles can be used for sensing other fluoroquinolones in biological samples that can be separated by capillary electrophoresis.

Acknowledgement The support of this research by Korea Research Foundation Grant (KRF-2004-005-C00009) is gratefully acknowledged.

References

1. McEvoy GK (ed) (2000) AHFS drug information. American Society of Health-System Pharmacists, Bethesda, MD
2. Squella JA, Alvarez-Lueje A, Sturm JC, Nunez-Vergara LJ (1993) Enoxacin: polarographic behavior and its determination in pharmaceutical forms. Anal Lett 26:1943–1957

3. Zhang ZQ, Li YF, He XM, Zhang H (1996) Electroanalytical characteristics of enoxacin and their analytical application. Talanta 43:635–641
4. Hamel B, Audran M, Costa P, Bressolle F (1998) Reversed-phase high-performance liquid chromatographic determination of enoxacin and 4-oxo-enoxacin in human plasma and prostatic tissue: Application to a pharmacokinetic study. J Chromatogr A 812:369–379
5. Hernández M, Borrull F, Calull M (2000) Determination of quinolones in plasma samples by capillary electrophoresis using solid-phase extraction. J Chromatogr B 742:255–265
6. Vyncht GV, Jánosi A, Bordin G, Toussaint B, Rogister GM, De Pauw E, Rodriguez AR (2002) Multiresidue determination of (fluoro)quinolone antibiotics in swine kidney using liquid chromatography–tandem mass spectrometry. J Chromatogr A 952:121–129
7. Süslü İ, Tamer A (2002) Spectrophotometric determination of enoxacin as ion-pairs with bromophenol blue and bromocresol purple in bulk and pharmaceutical dosage form. J Pharm Biomed Anal 29:545–554
8. Vílchez JL, Araujo L, Prieto A, Navalón A (2004) Determination of ciprofloxacin and enoxacin in human serum samples by micellar liquid chromatography. Anal Chim Acta 516:135–140
9. Espinosa-Mansilla A, de la Peña AM, Gómez DG, Salinas F (2005) HPLC determination of enoxacin, ciprofloxacin, norfloxacin and ofloxacin with photoinduced fluorimetric (PIF) detection and multiemission scanning: Application to urine and serum. J Chromatogr B 822:185–193
10. Chen S-I, Ding F, Liu Y, Zhao H-C (2006) Electrochemiluminescence of terbium (III)-two fluoroquinolones-sodium sulfite system in aqueous solution. Spectrochim Acta A 64(1):130–135
11. Yi L, Zhao H, Chen S, Jin L, Zheng D, Wu Z (2003) Flow-injection analysis of two fluoquinolones by the sensitizing effect of terbium(III) on chemiluminescence of the potassium permanganate–sodium sulfite system. Talanta 61:403–409
12. Karim MM, Lee SH, Lee HS, Bae ZU, Choi KH (2006) A batch chemiluminescence determination of enoxacin using a tris-(1, 10-phenanthroline) ruthenium(II)-Cerium(IV) system. J Fluoresc 16 (4):535–540
13. Karim MM, Jeon CW, Lee HS, Alam SM, Lee SH, Choi JH, Jin SO, Das AK (2006) Simultaneous determination of acetylsalicylic acid and caffeine in pharmaceutical formulation by first derivative synchronous fluorimetric method. J Fluoresc 16:713–721
14. Karim MM, Lee HS, Kim YS, Bae HS, Lee SH (2006) Analysis of salicylic acid based on the fluorescence enhancement of the arsenic (III)-salicylic acid system. Anal Chim Acta 576:136–139
15. Karim MM, Lee SH, Kim YS, Bae HS, Hong SB (2006) Fluorimetric determination of Ce(IV) with ascorbic acid. J Fluoresc 16:17–22
16. Karim MM, Alam SM, Lee SH (2007) Spectrofluorimetric estimation of norepinephrine using ethylenediamine condensation method. J Fluoresc 17:427–436
17. Espinosa-Mansilla A, de la Peña AM, Salinas F, Gómez DG (2004) Partial least squares multi component fluorimetric determination of fluoroquinolones in human urine samples. Talanta 62:853–860
18. You F, Jin L, Zhao H (1999) Study on fluorescence of the Tb(III)–enoxacin system and the determination of enoxacin. Anal Commun 36:231–233
19. Wang L, Wang LY, Zhu CQ, Wei XW, Kai XW (2002) Preparation of functionalized nanoparticles of cadmium sulfide as a fluorescence probe. Anal Chim Acta 468:35–41
20. Schmidt G, Malwitz MM (2003) Properties of polymer–nanoparticle composites. J Colloid Interface Sci 8(1):103–108
21. Bhattacharjee B, Ganguli D, Chaudhuri S (2002) Growth behavior of CdS nanoparticles embedded in polymer and sol-gel silica matrices: Relationship with surface-state related luminescence. J Fluoresc 12(3/4):369–375
22. Wang L, Chen H, Wang L, Li L, Xu F, Liu J, Zhu C (2004) Preparation and application of a novel composite nanoparticle as a protein fluorescence. Anal Lett 37(2):213–223
23. Alivisatos AP (1996) Perspectives on the physical chemistry of semiconductor nanocrystals. J Phys Chem 100(31):13226–13239
24. Alivisatos AP (1996) Semiconductor clusters, nanocrystals, and quantum dots. Science 271(5251):933–937
25. Panigrahi BS (2002) A fluorimetric study of terbium, europium and dysprosium in aqueous solution using pyridine carboxylic acids as ligands. J Alloy Comp 334(1–2):228–231
26. Zheng Y, Lin J, Liang Y, Lin Q, Yu Y, Guo C, Wang S, Zhang H (2002) A novel terbium (III) beta-diketonate complex as thin film for optical device application. Mater Lett 54:424–429
27. Wang Q-M, Yan B (2004) Novel luminescent molecular-based hybrid organic–inorganic terbium complex covalently bonded materials via sol-gel process. Inorg Chem Commun 7(6):747–750
28. Zhang N, Tang S-H, Liu Y (2003) Luminescence behavior of a water soluble calix[4]arene derivative complex with terbium ion (III) in gelation solution. Spectrochim Acta A 59(5):1107–1112
29. Suslick KS (ed) (1988) Ultrasound: its chemical, physical and biological effects. VCH, Weinheim, Germany
30. Wang L, Bian G, Dong L, Xia Y, Hong S (2005) Preparation of a novel fluorescence probe of terbium composite nanoparticles and its application in the determination of ascorbic acid. Microchim Acta 150:291–296
31. Suslick KS, Hammerton DA, Cline RE (1986) Sonochemical hot spot. J Am Chem Soc 108:5641–5642
32. Rieutord A, Vazquez L, Soursac M, Prognon P, Blais J, Bourget Ph, Mahuzier G (1994) Fluoroquinolones as sensitizers of lanthanide fluorescence: application to the liquid chromatographic determination of ciprofloxacin using terbium. Anal Chim Acta 290(1–2):215–225
33. Parker CA, Rees WT (1960) Correction of fluorescence spectra and measurement of fluorescence quantum efficiency. Analyst 85:587–600
34. Richardson FS (1982) Terbium(III) and europium(III) ions as luminescent probes and stains for biomolecular systems. Chem Rev 82:541–552
35. Lakowicz JR (1983) Principles of fluorescence spectroscopy. Plenum, New York, p 303
36. Bian W, Wang Y, Zhu X, Jiang C (2006) Spectrofluorimetric determination of trace amount of coenzyme II using ciprofloxacin–terbium complex as a fluorescent probe. J Lumin 118:186–192
37. Hercules DM (1966) Fluorescence and phosphorescence analysis, chap. 2. Interscience, New York